

A Platform for Experiments with Energy Storage Devices for Low-power Wireless Networks

Robert Hartung*

Jan Käberich

Lars C Wolf

{hartung|kaeberic|wolf}@ibr.cs.tu-bs.de

Technische Universität Braunschweig

Laura Marie Feeney*

Christian Rohner

Per Gunningberg

{lmfeeney|christian.rohner|perg}@it.uu.se

Uppsala University

ABSTRACT

We present a hardware platform for performing experimental studies of energy storage devices for low power wireless networks. It is based on a low-cost custom card that can apply fine-grain synthetic loads – both charge and discharge – to a set of batteries or capacitors and measure their response in detail. Loads can be defined from a “live” trace of a running wireless device, from a recorded trace, or programmatically via a script. This approach makes it practical to run well controlled, large scale, long running experiments and to obtain high precision and accuracy. We describe two proof-of-concept experiments using rechargeable Li coin cells and capacitors to demonstrate the capabilities of our platform.

CCS CONCEPTS

• **Networks** → **Network performance evaluation**; • **Hardware** → **Batteries**;

ACM Reference Format:

Robert Hartung, Jan Käberich, Lars C Wolf, Laura Marie Feeney, Christian Rohner, and Per Gunningberg. 2018. A Platform for Experiments with Energy Storage Devices for Low-power Wireless Networks. In *12th International Workshop on Wireless Network Testbeds, Experimental Evaluation & Characterization (WiNTECH '18)*, November 2, 2018, New Delhi, India. ACM, New York, NY, USA, 9 pages. <https://doi.org/10.1145/3267204.3267208>

*Both authors contributed equally to the paper

Permission to make digital or hard copies of all or part of this work for personal or classroom use is granted without fee provided that copies are not made or distributed for profit or commercial advantage and that copies bear this notice and the full citation on the first page. Copyrights for components of this work owned by others than ACM must be honored. Abstracting with credit is permitted. To copy otherwise, or republish, to post on servers or to redistribute to lists, requires prior specific permission and/or a fee. Request permissions from permissions@acm.org.

WiNTECH '18, November 2, 2018, New Delhi, India

© 2018 Association for Computing Machinery.

ACM ISBN 978-1-4503-5930-6/18/11...\$15.00

<https://doi.org/10.1145/3267204.3267208>

1 INTRODUCTION

Low-power wireless networks must be extremely energy efficient in order to obtain the long operational lifetimes needed for practical deployment. To achieve this, the community has mostly focused on developing protocols and applications that minimize the energy consumed by the devices.

Energy consumption is generally evaluated using “coulomb counting”. In some cases, specialized hardware is used to directly measure the current consumed by a running device. More commonly, a simulation (or the OS on a running device) is instrumented to track the operating state of various hardware components, such as the radio. Each state is associated with a known current consumption, creating a trace of the estimated current consumption over time. The charge consumed is the integral of the measured or estimated current over time.

The energy store itself – usually a small battery or a supercapacitor – has received much less attention. It is generally modeled as a simple ledger that tracks the remaining charge. Current consumption removes charge from the energy store and recharging replaces it. A device is assumed to fail when its energy store is depleted.

In reality, batteries and supercapacitors are complex electrochemical systems and exhibit non-linear behavior. Battery lifetime¹ depends heavily on the timing and magnitude of the applied load, as well as on external factors like temperature [9]. Two key properties are rate-dependent capacity (a lower current obtains a disproportionately longer lifetime than a higher one) and charge recovery (an intermittent load obtains a disproportionately longer lifetime than a continuous one). The latter is especially interesting because most low power devices operate with a low duty-cycle.

When a load is applied, the battery’s output voltage drops immediately and then continues to decrease over the duration of the load. When the load is removed, the output voltage partially recovers. This behavior depends on the magnitude and duration of load, the battery state-of-charge, and other factors such as temperature. A device fails, not when the

¹For brevity, the discussion here focuses on battery discharge.

battery has “run out of charge”, but when it is no longer able to maintain a sufficiently high output voltage under load.

This suggests that it is important to better understand the energy store in the context of low-power wireless devices. Earlier measurement studies, including [2], suggest that non-linear battery effects are potentially significant. Moreover, battery models have generally been directed towards larger, more complex batteries. Low-power wireless devices generally use low-cost single-cell batteries and the typical usage pattern is a relatively high current (up to a few 10's of mA), very low duty-cycle load with load durations on the order of a few ms to 1 s. Earlier studies suggest that this scenario is not well served by existing battery models [11]. However, the applicability of these results has been somewhat limited, due to limitations of existing testbeds.

The contributions of this work are (i) to define the requirements for an experimental platform that addresses low-power wireless network scenarios, (ii) to describe both the high-level approach and the low-level design decisions that allow us to meet them, and (iii) to characterize the performance of the implemented solution.

The main requirement is that the platform must support high quality, controlled experiments for measuring the physical processes in the energy store. At the same time, it is not a battery testbed *per se*; the goal is to provide meaningful information to developers of low-power wireless networks. The platform must somehow capture the essential behavior of a low-power wireless network and flexibly support investigations on a wide range of topics, from protocol optimization to network lifetime prediction.

Our platform achieves this by separating measurement of the energy store from the operation of the wireless devices that create load. It is based on a low-cost custom card that can apply fine-grain synthetic loads – both charge and discharge – to a set of batteries or supercapacitors and measure their response in detail. The cards are controlled via USB or Ethernet and are individually addressable. This approach has several advantages:

One, synthetic loads are fully controlled and reproducible. The platform provides several ways to define highly realistic loads, using live or recorded traces of running devices. In addition, a scripting interface allows loads to be defined programatically, such as from a simulation. Scripting also allows for stylized loads, which are useful in developing analytic battery models. Measurements can also be scripted to coordinate with the applied load and manage the amount of data collected.

Two, specialized hardware enables instrumenting the energy store more effectively than it is possible on an active wireless device. The test card is able to provide high resolution (up to 125kHz) measurements over short intervals. It also makes it possible to achieve very high accuracy and

precision. A smart calibration algorithm allows for component and temperature compensation, enabling precision and accuracy of 0.1 % + 1.5 mV and 0.3 % + 0.3 mA in voltage and current measurements, respectively. Temperature compensation is also essential when using the platform to study temperature-related effects.

Three, the platform is highly scalable. It is feasible to run large experiments, without the need for a long-running, large-scale wireless deployment. With a single rack of test cards, it is easy to run several independent experiments simultaneously, each using a statistically large number of batteries, over a period of weeks or even months. Furthermore, experiments can be performed under controlled environmental conditions, such as in a climate chamber.

Four, because the scripting and data collection interface runs on a PC and can be integrated into larger simulation or testbed control frameworks, there is considerable flexibility in how experiments are designed. The platform enables a wide variety of investigations, including protocol performance analysis, battery modeling, temperature effects, and lifetime prediction.

The outline of the paper is as follows: The test platform is presented in section 2, along with a characterization of its performance in section 3. Two proof-of-concept experiments are presented in section 4. Related work is discussed in section 5.

2 PLATFORM

The card is shown in Figure 1. Figure 1a shows the top view of the card. Eight battery holders for CR2032 coin cells are placed on the left hand side with additional pin headers for other types of storage devices. On the right, the data interfaces and power supply in the form of a USB-B and Ethernet can be seen. Furthermore, a jack is used for additional power when charging batteries. Three LEDs indicate status, error and busy operation.

The bottom of the card is shown in Figure 1b. Located below the eight battery holders are the analogue parts for draining or charging the batteries. The processor (STM32F407) and the digital parts for the remaining features, such as memory, voltage regulation, a temperature sensor and Power-over-Ethernet are located on the bottom as well which makes it easy to manufacture.

Figure 2 illustrates the high-level architecture of our platform. The two data interfaces are shown on the left and explained in detail in subsection 2.1.1. Eight independent channels for either eight batteries or super capacitors are available. The Analog Digital Converter (ADC) is used to read back voltage/current from each channel. The Digital Analog Converter (DAC) is used to control voltage and current for charging and discharging each channel.

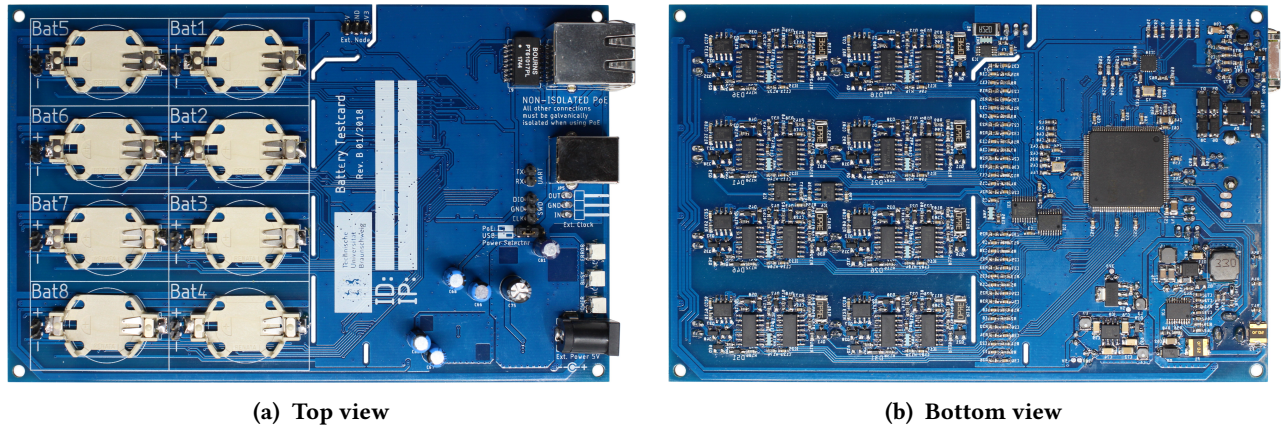


Figure 1: Images of the battery test card.

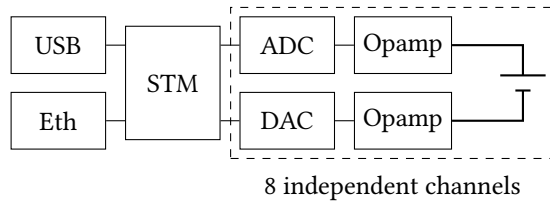


Figure 2: Illustration of the card's components and data interfaces

2.1 Features

In this section we present some key features of the card and map them back to the initial requirements.

2.1.1 Data Interfaces (PoE and USB). Two data interfaces have been implemented to make the card practical and easy to use. When using the card locally to a computer, it can be connected via USB. However, when running larger experiments with numerous test cards, USB is limiting the data rate. Also, a large number of USB hubs would be required. Therefore, an Ethernet connector with Power-over-Ethernet (PoE, IEEE 802.3af) capability was chosen as an alternative data interface. The card can then be connected to any regular PoE switch. The advantage is that a larger power budget is available with PoE, and the data rate being achieved is a lot higher, as we will show in later experiments (see section 4).

2.1.2 High Resolution Sampling. For battery modeling, high resolution sampling is required in order to derive parameters such as time constants of battery-internal capacitance and resistance, or to create fine-grain models supporting characteristic IoT loads [11]. For this purpose, a detailed battery-response which is measured by the voltage over time is very important. The sampling rate is limited by the

communication interface. Rates up to 125 kHz are obtained using Ethernet.

2.1.3 Sequence mode. For generating different load sequences on the card, we developed a high-level scripting language. These sequences are used for both charging and discharging the battery. A simple pattern with a current of 20 mA and a duty cycle of 10 % can be defined like this:

```
load 20mA, 100ms
load 0mA, 900ms
start
```

This would only apply the pattern to the batteries, but not log any data. Therefore, measurements and traces can be taken. Measurements are short samples at specific points in time and are used for long-term experiments (usually weeks or months):

```
load 20mA, 100ms
load 0mA, 900ms
measurement 0s
start
```

This would record the voltages at the beginning of the load on each channel. Another feature is to generate traces. It can be used to record high resolution data as presented above. The time within the sequence, the sample frequency and its duration have to be defined:

```
sampling 10kHz
load 20mA, 100ms
load 0mA, 900ms
measurement 0s
trace 0s, 0.5s
start
```

2.1.4 Live mode & playback mode. In addition to user defined scripts, the card also supports a live mode. An interface on the card can be connected to an external device, track its current consumption, and apply it to the batteries. These traces can also be stored and replayed (playback mode) or be generated from simulation tools. This feature allows, for example, to apply the same load to different types of batteries or at different temperatures.

2.1.5 Accuracy. All three modes for describing the load on the battery are defined in terms of current, which must be controlled as accurately as possible. The current control is therefore realized by using operational amplifiers. Besides improved accuracy, a compensation for errors due to temperature and noise is possible as well. Both accuracy and high resolution sampling cover the requirement of in-depth analysis of batteries in certain scenarios.

2.2 Design Decisions

Several design decisions have been made to fulfill the requirements. Our approach separates the measurement of the wireless devices and the discharge behavior of the battery. The following paragraphs highlight a few of the challenges we were facing and how we solved them.

Our platform should provide trustworthy measurement data for the requirements as presented in the introduction. An important parameter affecting the performance for batteries as well as for electronics is temperature. For batteries such as the common CR2032 coin cell, for re-chargeable batteries and for supercapacitors, experiments focusing on the impact of temperature was a designated feature. The different temperatures we generate for the system under test also could effect the platform itself. Placing and choosing components for the test platform itself was therefore an important design aspect. Our approach was along three lines; (i) the components themselves were chosen carefully with respect to their temperature coefficient, (ii) we avoid placing heat generating electronics next to sensitive components and batteries, and (iii) we implement temperature compensation in software.

Figure 3 shows the infrared picture of the battery card under operation. The two primary heat sources are the voltage regulators and the PoE parts. They are placed as far from the batteries as possible and separated from the batteries and the channel electronics by cutouts in the PCB that further reduce heat dissipation. The figure shows that the temperature difference among the batteries is about 1 °C, which is tolerable. The PCB around the batteries, where the channel drivers and measurement probes are placed, is only slightly above ambient temperature. Also a temperature sensor is placed in that part of the card to allow for temperature logging and compensation.

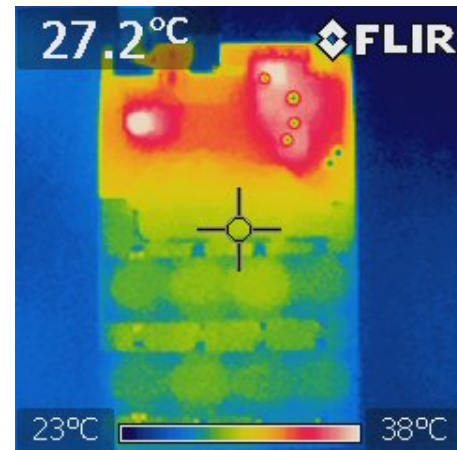


Figure 3: Infrared picture of the battery card showing different temperatures across the PCB.

3 PERFORMANCE CHARACTERIZATION

For every measurement device, two terms are very important when it comes to performance characterization: accuracy and precision. *Accuracy* describes a systematic error, e.g. an error between the actual value and the measured value. *Precision* describes the statistical variability around the measured value. A practical approach to achieve high precision is to reduce noise in the system and provide high resolution measurement and control components, such as ADCs and DACs. For accuracy, a calibration is required, which we will present in the next section.

3.1 Calibration

Calibration is required to compensate errors from the various analogue components that introduce errors. These errors can be categorized in linear and non-linear errors. The worst case of non-linear errors caused by the ADCs and DACs is about 3 LSB (Least Significant Bit). In contrast, the linear errors from all components, including shunt resistors and voltage offsets, are up to 50 LSB. Therefore, we concentrate on compensating linear errors. The linear errors can be further split into gain and offset errors. Both of these errors can be compensated by calibration. [12]

The complexity of our platform is that we have eight independent sub-systems (the output stages controlling the batteries) that all have to be calibrated separately. Additionally, to be able to achieve a good accuracy in temperature experiments, a calibration at different ambient temperatures is required as well. For compensating the linear errors, two calibration points are required for every ADC and DAC. Given that both current and voltage measurement have to be calibrated, manually setting individual calibration points was not a viable option. Instead, a simple lab power supply with

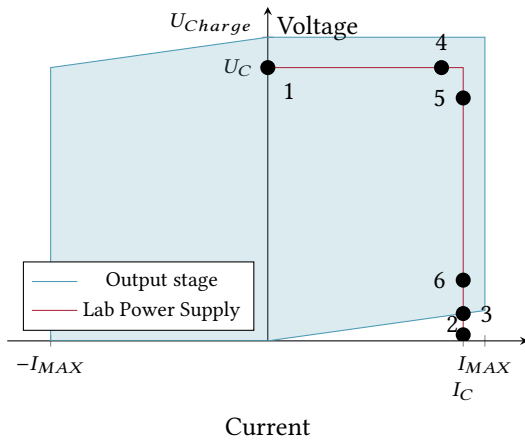


Figure 4: Operating areas and used calibration points

both a voltage and current limit is used for this process. By limiting both the voltage and current to a known value (U_C and I_C), we can calibrate the whole test platform within one single calibration process. The lab power supply is connected to all eight output stages in parallel.

3.1.1 Calibration method. To describe the calibration process, we have to briefly introduce the design of each output stage. Each output stage can read voltage and current using an ADC and force the current or limit the voltage using a DAC. We can use this design together with the limits of the lab power supply to drive the operation point to a few selected points. Figure 4 shows the operation points used for calibration which we will present shortly:

Point 1 is recoding the first calibration point for both the voltage and current ADC as well as the current DAC. The hardware supports sign detection of the current, making it possible to zero the DAC (to within 1 LSB). As no current flows through *all* of the output stages, the voltage is known due to the lab power supply.

Point 2 draws the maximum current in all output stages and therefore forcing the voltage of the lab power supply close to 0 V. This represents the second and final calibration point for the voltage ADC and enables the system to accurately measure voltages. Calibrating the current ADC in this step is not possible, as the current is not necessarily distributed equally among the output stages.

Point 3 is similar to Point 2 except that only a single output stage is active, thus a current of I_C flows through the stage and the calibration of the current ADC is complete. To calibrate all eight current ADCs, this and all subsequent steps are repeated for each output stage.

Point 4 forces a current slightly below I_C . The actual current flowing can be measured using the ADC (as it is already fully calibrated), sampling the second calibration point for the current DAC.

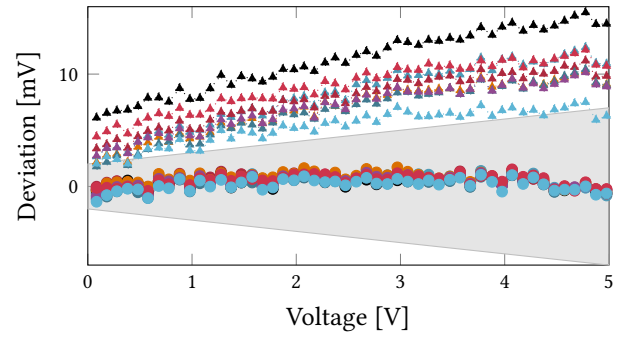


Figure 5: Deviation of the voltage before (triangle) and after (circle) the calibration.

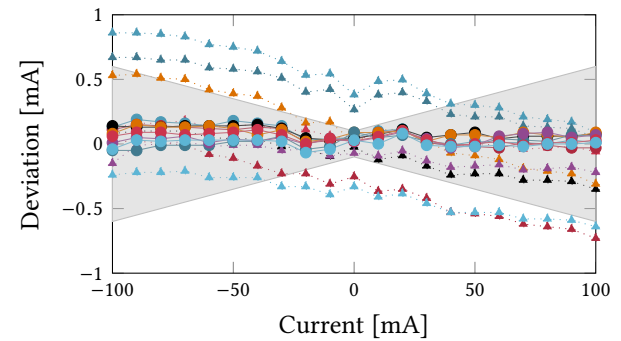


Figure 6: Current deviation without and with calibration

Points 5 & 6 are similarly used to calibrate the voltage DAC by choosing points close to the edges of the operating range and sampling the actual voltage with the already calibrated ADC.

3.1.2 Calibration results. Figure 5 and Figure 6 show both the voltage and current readings before and after our calibration for the eight power sources (i.e., batteries). The gray area marks the accuracy of our multimeter that we used as reference. The lines with triangle markers show the deviation before the calibration and lines with circles after we applied the calibration. In general, after the calibration process both the voltage and current readings are well within and even below our reference's accuracy with 2 mV and 0.5 mA. As a further indication, the measurements among the different batteries are much more consistent than without calibration.

3.1.3 Calibration results for temperature. As the battery platform will be used for temperature experiments, calibration is repeated at different temperatures. Figure 7 shows the maximum deviation of the current across the temperature range between 0 °C and 50 °C. The maximum delta of 0.26 mA is only 0.25 % error, relative to our current range of 150 mA.

Table 1: Testcard specifications

| Parameter | | Min | Typ | Max | Unit |
|------------------------|--------------------------|--------|---------|---------|---------|
| Voltage range | | 0 | | 5 | V |
| Native resolution | | | 1.22 | | mV |
| Oversampled resolution | | 0.1 | | 1.22 | mV |
| Accuracy | T=0 °C to 50 °C | | 0.05+1 | 0.1+1.5 | %+mV |
| Current range | $R_{Shunt} = 3.9 \Omega$ | -106.8 | | 106.8 | mA |
| Resolution | $R_{Shunt} = 3.9 \Omega$ | | 52.16 | | μA |
| Accuracy | with calibration | | 0.2+0.2 | 0.3+0.3 | %+mA |

| Parameter | | Min | Typ | Max | Unit |
|--------------------------------------|--|------------|------------|------------|-------------------|
| USB (PoE) charge current per channel | | | | -25 (-125) | mA |
| USB (PoE) continuous sampling rate | | | | 25 (125) | kHz |
| USB (PoE) measurement noise | | 0.13 (0.2) | | 3.2 (7.2) | mV _{RMS} |
| USB (PoE) set current noise | | | 0.05 (0.5) | | mA _{RMS} |

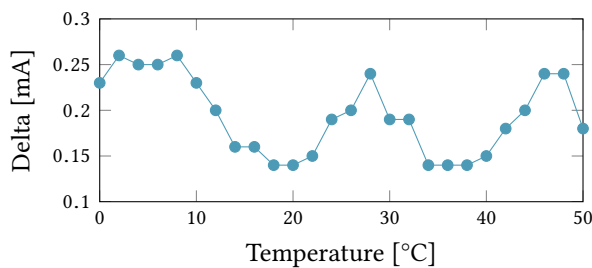


Figure 7: Maximum deviation of the current across the whole temperature range

3.2 Current Control Accuracy

To evaluate the accuracy of the output stage to control the load applied to a power source, we look at the step response when switching from charging (negative current) to discharging (positive current). This scenario is the most challenging because we have to make sure to never be in both modes at the same time and because the closed-loop design to set the desired target current needs some time to settle. The design of the control system uses opAmps in the feedback path to sense current and voltage. While this enables cheap and accurate results it also has a few trade-offs. First, additional phase shift is introduced. To keep the system stable, the gain has to be limited, for which a relatively large resistor R in the feedback path would be desirable. Second, switching direction of the current requires to overcome the blocking range of the output driver (non-biased push-pull-stage), during which no current can flow. This period of time is proportional to the above mentioned resistor in the feedback path, that is, a smaller value for resistor R would be desirable.

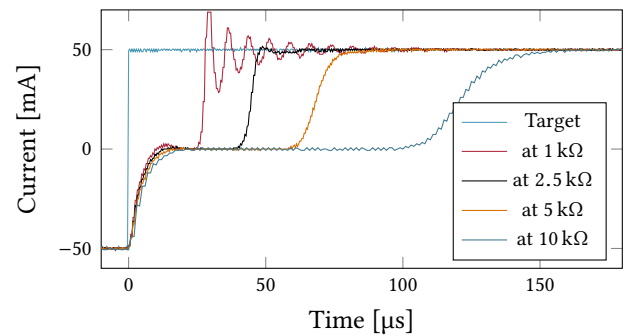


Figure 8: Step response with different signs and different resistors values within the control path.

Figure 8 shows the step response of the current control when using different values of R during a current sequence from -50 mA to 50 mA. Too small values of R introduce oscillation due to the limited phase margin of the control circuit, while larger values introduce a very small skew rate and result in slow control of the current. The exact value of R for which no oscillation is present depends on part tolerances and is slightly influenced by temperature. Therefore, we chose a conservative value of $R = 10$ k Ω in order to always have a stable control system. The subsequent slow step response is often acceptable as sign changes of the current are expected to be rare and the response to current steps without a sign change is significantly faster.

3.3 Card Specifications

Table 1 shows a brief overview of the cards specifications. Our native resolution is just 1.22mV which results from the

12 bit ADC. Without any calibration both the current and voltage accuracy are worse by the factor of 3.

Finally, the power source of the card has an impact on the battery card's performance. When powered from USB, the noise is reduced, and the sampling rate is limited. On the other hand, PoE offers a five-times higher sampling rate but introduces a lot more noise to current measurements.

4 EXPERIMENTS

To show the capability and usage of the test platform we have setup two proof-of-concept experiments. The first experiment shows the discharging behavior of very small Lithium-Ion (Li-ion) batteries. The second experiment shows an exemplary use case of characterizing supercapacitors.

4.1 Example: Rechargeable Batteries

This experiment was designed in the context of a study that tracks the movements of bats [1]. The tracking devices use very small Li-ion batteries. These batteries have a nominal capacity of only 22 mA h and they are used due to their extremely small weight, which is required to put them on the backs of bats. The idea is to maximize lifetime, by deeply discharging the batteries. Our experiment tries to find out how much more energy can be taken out of the batteries below its cutoff voltage. Therefore, the batteries are charged to the nominal voltage and then drained by a predefined application-specific pattern which covers both the duty-cycled send periods and the sleep current in between. Throughout the experiment, we record the voltage of each of the eight batteries, and read the cumulated energy for each battery since the beginning of the experiment. The results are shown in Figure 9 and show the normalized energy on the y axis and the cut off voltage on the x axis that can be taken from the batteries. Our experiments have shown that the energy varies by up to 10 %. Finally, our experiment indicates that most of the energy is already discharged at about 3.6 V and deep discharges below this voltage should be avoided to not damage the cell.

4.2 Example: Supercapacitors

Supercapacitors are an emerging technology to store energy generated by energy harvesting. Their advantage is their almost linear discharge behavior, which makes predicting remaining energy easier than for batteries. However, the stored energy can be fairly small and self-discharge can be a problem as well.

Figure 10 shows a set of supercapacitors that are connected to the pin headers of the platform. Using our platform we can charge and discharge supercapacitors and make the same experiments as for batteries. We can see effects of different

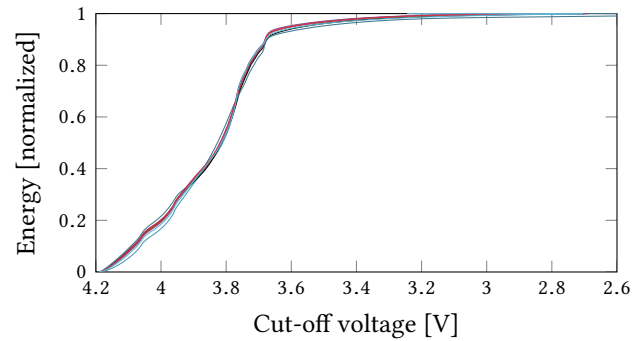


Figure 9: Discharged energy at different cut-off voltages

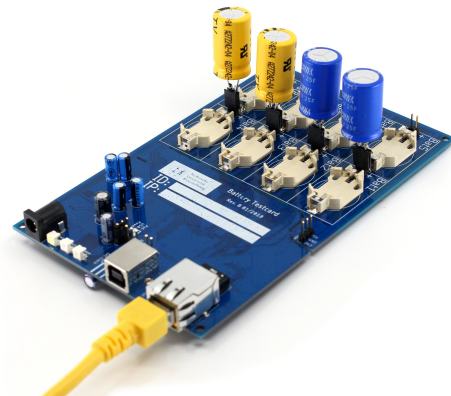


Figure 10: Using the test platform with supercapacitors

load patterns and temperature on the supercapacitor's stored energy.

We use eight identical capacitors with no stored energy at the beginning of the experiments. We charge them to 2.7 V and discharge them right afterwards to minimize self-discharging effects. Throughout this experiment, we sample both the current and voltage of the eight channels at a fixed interval.

Table 2 lists the capacitors with the calculated efficiency and capacity. The efficiency is the factor between the charged and discharged energy. The capacity can be calculated by $E = \frac{1}{2} \cdot C \cdot U^2$, as both E and U are known. The efficiency and capacity are comparable with other experiments on supercapacitors [10], while the capacity is a little higher with almost 50 % for all capacitors.

Characterizing the supercapacitors of a system is therefore extremely important, because the remaining energy in the supercapacitors can only be predicted, if the capacity is known precisely.

Table 2: Energy of different supercapacitors with $C_{nominal} = 1\text{ F}$

| Capacitor | Efficiency [%] | Capacity [F] |
|-----------|----------------|--------------|
| 1 | 69.3 | 1.44 |
| 2 | 67.6 | 1.44 |
| 3 | 67.2 | 1.53 |
| 4 | 69.0 | 1.52 |
| 5 | 69.0 | 1.42 |
| 6 | 69.2 | 1.46 |
| 7 | 68.5 | 1.44 |
| 8 | 66.8 | 1.46 |

5 RELATED WORK

This paper builds on an earlier testbed, which was used to collect extensive long-term measurements of primary Li coin cells (CR2032) being discharged using synthetic loads whose timing and current values were derived from typical sensor network operations [2]. The results clearly demonstrated the impact of non-linear effects, such as the rate-capacity effect and charge recovery. For example, simple linear calculations of battery lifetime were shown to err by up to a factor of three, for high-current, low duty-cycle loads.

This work was the first to support these kinds of experiments and eventually it became clear that the test cards (which were re-purposed from battery Q/A hardware) had a number of limitations. The platform described here is an entirely new design that achieves better precision and accuracy and supports a much wider range of experiment scenarios.

In particular, the original cards used a set of four resistors to define up to 15 different resistive loads, which meant that the current values were poorly controlled. By contrast, the new cards provide a current-controlled load with an accuracy of a few hundred μA . Furthermore, the original cards only measured the battery's response to an applied load at three points. On the new cards, measurements are scripted and can include both point measurements and samples measured at rates up to 125kHz. The ADC measurement resolution is 1.22 mV, compared to 11.2 mV for the original cards. Accuracy is further improved through an automated per-battery calibration mechanism.

There are a number of new features: The new cards can apply a negative (i.e. charging) load, enabling experiments with rechargeable batteries and supercapacitors. Loads can also be taken from a "live" or recorded trace of a real wireless device. In addition, the new cards are temperature compensated, a feature that first appeared in PotatoScope, part of our earlier experimental deployment of an agricultural sensor network [4]. Temperature compensation not only improves accuracy,

it also facilitates integration with temperature-controlled test environments.

More generally, there have been relatively few reported attempts to measure battery discharge behavior in the context of low-power wireless networks: Characterizations of a Li coin cell (CR2354) are reported in [7] and [8]. The non-linear rate-capacity and charge recovery effects are clearly visible in the results. But both experiments were based on manual measurements of a few batteries, connected to wireless devices operating at very high duty cycles. A characterization of AAA alkaline batteries reported in [5] has similar limitations. An experiment reported in [3] measured Li coin cell (CR 2032) performance under more realistic load patterns that were inspired by the operation of Bluetooth radios. The batteries were shown to handle high peak loads with a low duty cycle reasonably well, but the test environment does not appear to have supported large scale or more general experiments. An experiment to systematically measure the battery lifetime of devices operating in a real wireless environment is reported in [6]. But to keep the experiment duration practical, the loads needed to be very high. And because the loads could not be fully controlled, or even characterized in detail, it was not possible to draw many conclusions.

6 CONCLUSION AND FUTURE WORK

A better understanding of the role of energy storage devices is important for improving the lifetime of low-power wireless networks. This work describes a unique platform for performing long-running, large-scale experiments with energy storage devices. The platform is based on a low-cost custom card that can apply fine-grain synthetic loads to a set of batteries or capacitors and collect very high resolution measurements of the response. We also outline two proof-of-concept experiments, using rechargeable Li-ion coin cells and supercapacitors, respectively.

The platform will produce results that are well-suited to the needs of the wireless and embedded systems community due to its scalability, its ease and flexibility of defining realistic loads, and its high precision and accuracy, especially under varying temperature conditions. We expect it to enable a wide variety of experiments, including protocol design and performance analysis, battery characterization and modeling, and lifetime prediction under varying environmental conditions.

REFERENCES

- [1] Björn Cassens, Simon Ripperger, Martin Hierold, Frieder Mayer, and Rüdiger Kapitza. 2017. Automated Encounter Detection for Animal-Borne Sensor Nodes. In *Int'l Conf on Embedded Wireless Systems and Networks (EWSN)*.
- [2] Laura Marie Feeney, Christian Rohner, Per Gunningberg, Anders Lindgren, and Lars Andersson. 2014. How do the dynamics of battery

- discharge affect sensor lifetime?. In *11th IEEE/IFIP Conf on Wireless On-demand Network Systems and Services (WONS)*.
- [3] Kjartan Furset and Peter Hoffman. 2011. *High pulse drain impact on CR2032 coin cell battery capacity*. Nordic Semiconductor and Energizer. Technical memo.
- [4] Robert Hartung, Ulf Kulau, and Lars C Wolf. 2016. Distributed Energy Measurement in WSNs for Outdoor Applications. In *IEEE Int'l Conf on Sensing, Communication and Networking (SECON)*.
- [5] Konstantin Mikhaylov and Jouni Tervonen. 2012. Experimental evaluation of alkaline batteries's capacity for low power consuming applications. In *IEEE 26th Int'l Conf on Advanced Information Networking and Applications (AINA)*.
- [6] Hoang Anh Nguyen, Anna Förster, Daniele Puccinelli, and Silvia Giordano. 2011. Sensor node lifetime: an experimental study. In *IEEE Int'l Conf. on Pervasive Computing and Communications Workshops (PERCOM Workshops)*.
- [7] Chulsung Park, Kanishka Lahiri, and Anand Raghunathan. 2005. Battery discharge characteristics of wireless sensor nodes: An experimental analysis. In *IEEE Conf. on Sensor and Ad-hoc Communications and Networks (SECON)*.
- [8] Sung Park, Andreas Savvides, and Mani B. Srivastava. 2001. Battery Capacity Measurement And Analysis Using Lithium Coin Cell Battery. In *Int'l Symp. Low Power Electronics & Design (ISLPED)*.
- [9] R. Rao, S. Vrudhula, and D.N. Rakhmatov. 2003. Battery modeling for energy aware system design. *IEEE Computer* 36, 12 (2003).
- [10] Christian Renner and Volker Turau. 2010. CapLibrate: Self-Calibration of an Energy Harvesting Power Supply with Supercapacitors.. In *ARCS Workshops*. 349–358.
- [11] Christian Rohner, Laura Marie Feeney, and Per Gunningberg. 2013. Evaluating Battery Models in Wireless Sensor Networks. In *11th Int'l Conf on Wired/Wireless Internet Communications (WWIC)*.
- [12] ST Microelectronics 2016. *STM32F407 MCU*. ST Microelectronics. <https://www.st.com/resource/en/datasheet/dm00037051.pdf>